# Induction of a Longer Term Component of Isoprene Release in Darkened Aspen Leaves: Origin and Regulation under Different Environmental Conditions[1]

**Bahtijor Rasulov, Katja Hüve, Agu Laisk, and Ülo Niinemets***

Institute of Molecular and Cell Biology, University of Tartu, 51010 Tartu, Estonia (B.R., A.L.); and Institute of Agricultural and Environmental Sciences, Estonian University of Life Sciences, 51014 Tartu, Estonia (K.H., Ü.N.)

After darkening, isoprene emission continues for 20 to 30 min following biphasic kinetics. The initial dark release of isoprene (postillumination emission), for 200 to 300 s, occurs mainly at the expense of its immediate substrate, dimethylallyldiphosphate (DMADP), but the origin and controls of the secondary burst of isoprene release (dark-induced emission) between approximately 300 and 1,500 s, are not entirely understood. We used a fast-response gas-exchange system to characterize the controls of dark-induced isoprene emission by light, temperature, and $CO_2$ and oxygen concentrations preceding leaf darkening and the effects of short light pulses and changing gas concentrations during dark-induced isoprene release in hybrid aspen (*Populus tremula* × *Populus tremuloides*). The effect of the 2-*C*-methyl-D-erythritol-4-phosphate pathway inhibitor fosmidomycin was also investigated. The integral of postillumination isoprene release was considered to constitute the DMADP pool size, while the integral of dark-induced emission was defined as the "dark" pool. Overall, the steady-state emission rate in light and the maximum dark-induced emission rate responded similarly to variations in preceding environmental drivers and atmospheric composition, increasing with increasing light, having maxima at approximately 40°C and close to the $CO_2$ compensation point, and were suppressed by lack of oxygen. The DMADP and dark pool sizes were also similar through their environmental dependencies, except for high temperatures, where the dark pool significantly exceeded the DMADP pool. Isoprene release could be enhanced by short lightflecks early during dark-induced isoprene release, but not at later stages. Fosmidomycin strongly suppressed both the isoprene emission rates in light and in the dark, but the dark pool was only moderately affected. These results demonstrate a strong correspondence between the steady-state isoprene emission in light and the dark-induced emission and suggest that the dark pool reflects the total pool size of 2-*C*-methyl-D-erythritol-4-phosphate pathway metabolites upstream of DMADP. These metabolites are converted to isoprene as soon as ATP and NADPH become available, likely by dark activation of chloroplastic glycolysis and chlororespiration.

Isoprenoids synthesized via the chloroplastic 2-*C*-methyl-D-erythritol-4-phosphate (MEP) pathway are important components of leaf photosynthetic machinery and serve as key lipid-soluble antioxidants and defenses against pathogens and herbivores (Mahmoud and Croteau, 2002; Cordoba et al., 2009; Rivasseau et al., 2009; Vickers et al., 2009). The simplest volatile isoprenoid, isoprene, plays a major role in protecting plants from heat (Sharkey and Singsaas, 1995; Behnke et al., 2007) and oxidative (Loreto and Velikova, 2001; Affek and Yakir, 2002) stresses and can also serve as a repellent for herbivores (Loivamäki et al., 2008). Plant-released isoprene is also the most important volatile hydrocarbon in the atmosphere, with major implications for ozone and secondary organic aerosol formation at scales ranging from regional to global (Fuentes et al., 2000; Claeys et al., 2004). Therefore, understanding the controls on the MEP pathway, and in particular on isoprene emissions, is of major fundamental and practical value in plant science, ecology, and atmospheric chemistry (Sharkey et al., 2008; Niinemets et al., 2010).

It is known that isoprene can be emitted light independently from many organisms, from microbes to humans (Deneris et al., 1985), but the release of isoprene from plant leaves is usually considered to be strictly light dependent, since energetic cofactors of the MEP pathway, ATP, CTP, and NADPH, are considered to be of photosynthetic origin (Monson and Fall, 1989; Loreto and Sharkey, 1990; Sharkey et al., 2008). However, postillumination isoprene emission continues for several minutes into darkness at the expense of the accumulated pool of the immediate isoprene substrate, dimethylallyldiphosphate (DMADP), and likely to a lesser extent of isopentenyl diphosphate (IDP), which is in equilibrium with DMADP (Rasulov et al., 2009a, 2009b, 2010; Li et al., 2011). After exhaustion of this pool

[1] This work was supported by the Estonian Ministry of Education and Science (grant nos. SF1090065s07 and SF0180045ds08), by the Estonian Science Foundation (grant nos. 7272, 7645, and 8283), and by the Human Frontier Science Program.

* Corresponding author; e-mail ylo.niinemets@emu.ee.

The author responsible for distribution of materials integral to the findings presented in this article in accordance with the policy described in the Instructions for Authors (www. plantphysiol.org) is: Ülo Niinemets (ylo.niinemets@emu.ee).

www.plantphysiol.org/cgi/doi/10.1104/pp.111.176222

of immediate isoprene precursors, postillumination isoprene release initially stops, but a secondary burst of isoprene emission is induced in 5 to 10 min after leaf darkening (dark-induced emission; Monson et al., 1991; Rasulov et al., 2010; Li et al., 2011). This secondary burst of isoprene emission lasts commonly tens of minutes (Monson et al., 1991; Rasulov et al., 2010; Li et al., 2011), and its magnitude and timing depend on temperature (Li et al., 2011).

Given that the key enzyme for isoprene emission, isoprene synthase, is only present in chloroplasts (Silver and Fall, 1995; Vickers et al., 2010), the existence of a secondary burst of isoprene emission raises several fundamental questions about the MEP pathway and isoprene emission regulation in chloroplasts. First, is the chloroplastic MEP pathway activated in the dark, resulting in isoprene release? Given that the chloroplastic pools of ATP and NADPH can support photosynthesis for only a few seconds in the dark (Sharkey et al., 1986; Pearcy, 1988; Ruuska et al., 1998), how are the necessary carbon skeletons and energetic cofactors of the MEP pathway produced in the absence of photosynthesis? Can chloroplastic glycolysis and chlororespiration energetically support the dark-induced isoprene emission (Loreto et al., 2000)? Or does the activation of the secondary isoprene release reflect a transfer of isoprenoid precursors, DMADP and IDP, into the chloroplast from the cytosol (Schwender et al., 2001; Bick and Lange, 2003; Rodríguez-Concepción, 2006)?

Based on the temperature kinetics of light and dark release of isoprene emission, Li et al. (2011) hypothesized that dark-induced isoprene emission reflects the total pool size of the MEP pathway upstream of DMADP. In this study, we used an ultrafast gas-exchange system to compare the responses of the steady-state isoprene emission in light and the maximum dark-induced isoprene emission to light, temperature, ambient $CO_2$, and oxygen and applied the inhibitor of the MEP pathway, fosmidomycin, to gain insight into the origin and regulation of dark-induced isoprene emission in hybrid aspen (*Populus tremula* × *Populus tremuloides*). Different from the oak (*Quercus* spp.) studied by Li et al. (2011), aspen is characterized by strong $CO_2$ sensitivity of steady-state isoprene emission (Rasulov et al., 2009b). The results of our study indicate close coordination of dark-induced isoprene emission with steady-state isoprene emission and support the control of the dark-induced emission by the total pool size of MEP pathway metabolites upstream of DMADP. We suggest that the dark-induced isoprene emission reflects the continuation of the photosynthetically supported MEP pathway in the dark, after a lag time necessary for the reversal of the glycolytic part of the pentose phosphate carbon reduction cycle toward the catabolic direction. Overall, the results of this study suggest that the kinetics of dark release of isoprene emission provide a highly valuable tool for gaining fundamental insight into the regulation of the MEP pathway in chloroplasts in vivo.

## RESULTS

### Postillumination and Dark-Induced Isoprene Emission: General Patterns

After switching off the light, the isoprene emission rate approaches a minimum at about 300 s after the darkening and then increases again (Fig. 1). The following kinetics of induced isoprene emission in the dark depend on temperature. Under 33°C, used as the standard temperature in most of the experiments reported here, the emission proceeds through a maximum at about 700 s after darkening and decays to zero at about 1,300 to 1,400 s. Such a dark isoprene emission lasting for about 20 to 25 min was observed in all experiments. In the following, the first process, completed within 200 to 300 s, is referred to as the postillumination isoprene emission. The subsequent longer term process is defined as the dark-induced isoprene emission.

The declining transient of postillumination isoprene emission up to approximately 200 to 300 s after switching off the light relies on the existing DMADP pool (with some minor contribution of IDP), and the whole integral of the isoprene release during this period equals the total DMADP pool size responsible for steady-state isoprene emission during light (see Eq. 1 below). Integrating the pool from a certain time $t$ to cessation of the fast isoprene release process [$S_{DMADP}(t)$; Eq. 2) corresponds to the pool size responsible for the isoprene emission rate $I(t)$ sustained at that time point (Eq. 2). Thus, paired values of $I(t)$ versus $S_{DMADP}(t)$ constitute the in vivo kinetic curve of isoprene synthase (insets in Fig. 1). These kinetic curves approximated closely the first-order reaction with the rate constant, $k_a$, of approximately 0.02 $s^{-1}$ (Fig. 1). When light was turned on at the end of the dark emission (20–25 min in darkness), isoprene emission recovered to a previous steady-state level in 5 to 10 min.

### Effect of Short Light Pulses Given during Dark-Induced Isoprene Emission

After cessation of the postillumination isoprene release, illumination of leaves with white light pulses of 2 to 4 s immediately accelerated isoprene emission at the beginning of the dark-induced emission, approximately 350 s after leaf darkening (Fig. 1A), but had a minor effect at the time of the maximum of dark-induced emission approximately 700 s after darkening (Fig. 1B) and did not have any effect at the end of the dark-induced emission burst in approximately 1,300 to 1,500 s after darkening (data not shown). The DMADP pools corresponding to the light pulses given early and late during the darkening (Fig. 1) were much less than those corresponding to the steady-state isoprene emission during light. However, $k_a$ values were not affected at least for a time period of 700 s after darkening (Fig. 1A for a comparison of $k_a$ values between 100 and

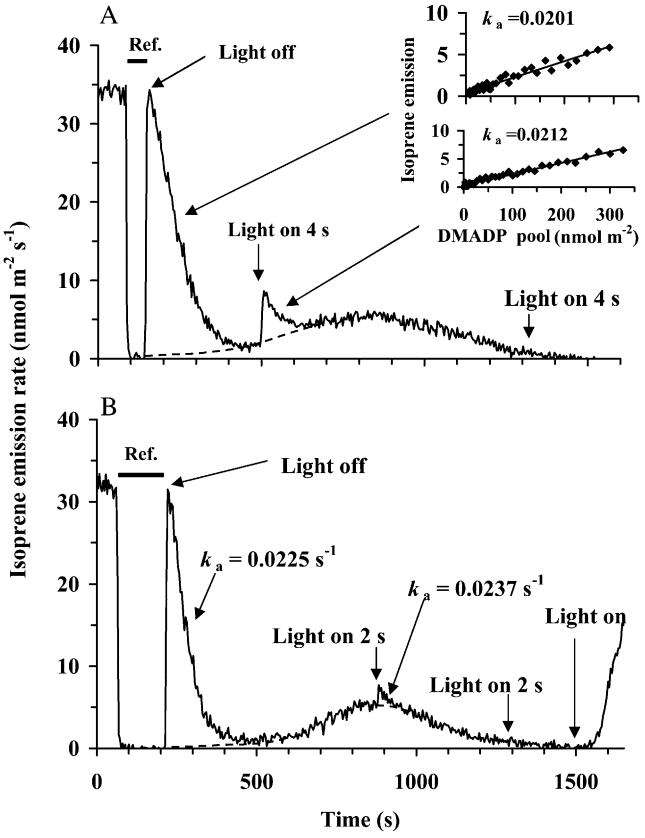


**Figure 1.** Illustration of the protocol for the measurement of steady-state isoprene emission rate of illuminated samples and transient isoprene release after rapid leaf darkening, and the effect of light pulses during the dark transient phase on isoprene emission in hybrid aspen. A fast two-channel gas-exchange system with a half-response time of 0.15 s was employed (Rasulov et al., 2010). The applied measurement protocol was similar for both the experiments in A and B, except for different timing of light pulses given in the darkness. In A, the recording begins in the steady-state conditions. At time 100 s, the reference line was recorded by switching between the reference and sample lines (shown by a horizontal bar). At 130 s, light was turned off, and the leaf chamber was simultaneously returned into the measurement channel. The following isoprene emission was recorded in the dark. In B, the steady-state isoprene emission rate in light is shown between 0 and 85 s, and the reference is measured between 85 and 210 s. The dotted line is the assumed activation time course of the dark-induced isoprene emission. The inset in A demonstrates an estimation of the rate constant of isoprene synthase ($k_a$; $s^{-1}$) for the periods 290 to 400 s and 500 to 600 s. The rate constant was determined from the relationships of isoprene emission rate ($I$) at time $t_1$ versus the pool size of DMADP remaining at $t_1$ (for further details, see Eq. 2 and Rasulov et al., 2010). The corresponding rate constants of isoprene synthase ($k_a$; $s^{-1}$) are also shown. In both experiments, quantum flux density during the light period was 600 $\mu$mol $m^{-2}$ $s^{-1}$, leaf temperature was maintained at 33°C, ambient $CO_2$ concentration at 360 $\mu$mol $mol^{-1}$, and oxygen concentration at 21%.

250 s after darkening and Fig. 1B for a comparison of $k_a$ values between 100 and 700 s after darkening), indicating that isoprene synthase activity was not altered during this time period.

### Effects of Light on Postillumination Isoprene Release and on the Intermediate Pools

In addition to the rate of steady-state isoprene emission in light, the maximum dark-induced isoprene emission increased with increasing quantum flux density (Fig. 2A). At different light intensities, the maximum of the dark-induced emission rate was approximately 10% to 20% of the preceding steady-state rate (Fig. 2A). The integral of the whole dark-induced

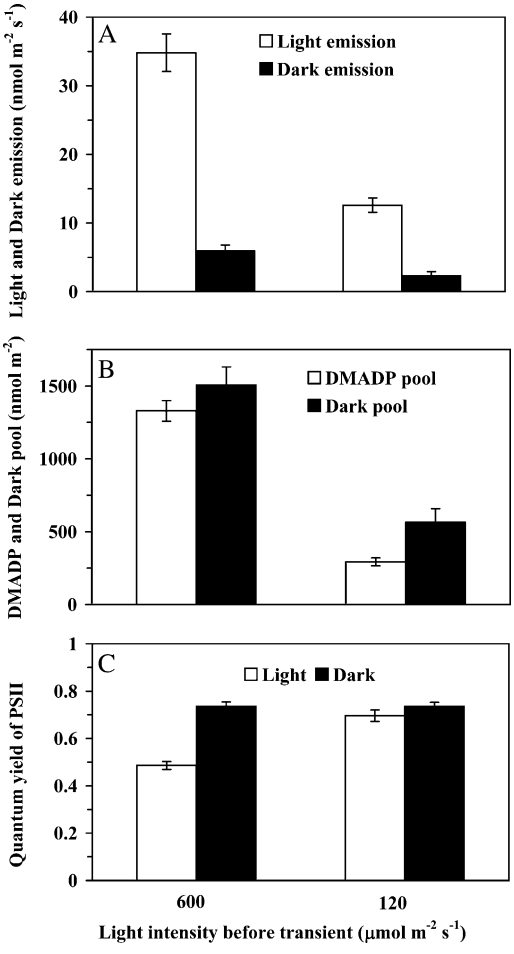


**Figure 2.** Influence of quantum flux density on the rates of steady-state isoprene emission in light and on the maximum dark-induced isoprene emission (A), DMADP pool size and dark pool size corresponding to these rates (B), and the light-adapted [$(F_m' - F)/F_m'$] and dark-adapted [$(F_m - F_0)/F_m$] quantum yields of PSII (C). The dark-induced emission is defined as the process induced after the fast dark transient of isoprene emission has relaxed, at approximately 300 to 400 s after switching off the light (for sample relationships, see Fig. 1). The DMADP pool is obtained by integrating the isoprene emission rate following the fast transient after switching off the light (up to approximately 200–300 after darkening), while the dark pool is obtained by integrating the emission transient activated in darkness (between approximately 300 and 1,500 s after switching off the light; Fig. 1). In these experiments, ambient $CO_2$ concentration was 360 $\mu$mol $mol^{-1}$, oxygen concentration was 21%, and leaf temperature was kept at 33°C. The data are averages ± SD of four independent experiments.

emission process (the dark pool) was numerically similar to the DMADP pool (postillumination) at high light (Fig. 2B). Both the dark pool and the DMADP pool decreased with decreasing light, but the dark pool remained at a somewhat higher level in low light (Fig. 2B). The effective quantum yield of PSII was reduced at higher light as photosynthetic electron transport approached saturation, whereas the dark-adapted quantum yields were not affected by incident light, demonstrating the absence of photoinhibition (Fig. 2C).

### $CO_2$ Responses of Isoprene Emission and Intermediate Pools in Light and Dark

The steady-state rate of isoprene emission in light exhibited a maximum at a low $CO_2$ concentration close to the $CO_2$ compensation point and decreased toward lower and higher $CO_2$ concentrations. The maximum dark-induced emission rate behaved very similarly (Fig. 3A), and both emission rates were strongly correlated (Fig. 3A, inset). In fact, throughout the $CO_2$ response curve, the ratio of the maximum dark-induced emission to emission in light was essentially constant at different $CO_2$ concentrations, averaging 0.161 ± 0.008. The pool sizes supporting the steady-state emission and the dark-induced isoprene emission were numerically also very similar and changed in the same manner with changing $CO_2$ concentration (Fig. 3B). Changing the $CO_2$ concentration in the dark had no effect on the dark-induced isoprene emission (data not shown). Quantum yields of PSII increased with increasing $CO_2$ concentration (Fig. 3C). Quantum yields measured in the dark 5 to 6 min after darkening demonstrated that the nonphotochemical quenching partly remained, in particular under lower $CO_2$ concentrations (Fig. 3C).

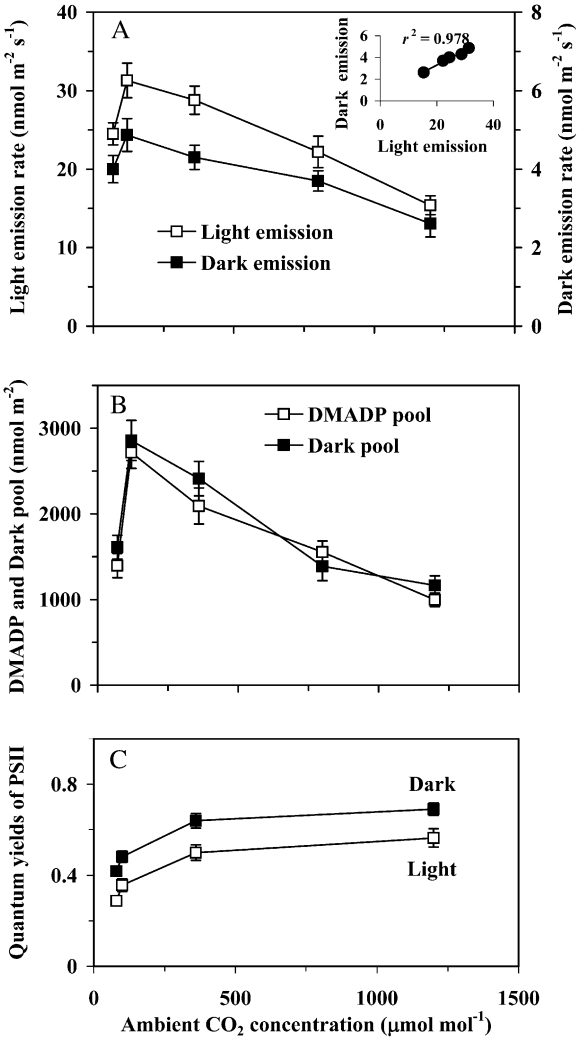


**Figure 3.** Effects of ambient $CO_2$ concentration on the rates of steady-state isoprene emission in light and on the maximum dark-induced emission rate (A), the pool of DMADP corresponding to the steady-state isoprene emission rate and the dark pool corresponding to the dark-induced emission (B), and the quantum yield of PSII in light and in dark (C). In the case of quantum yield in the dark, the measurements were conducted 5 to 6 min after darkening, and the maximum fluorescence had not yet fully relaxed. Term definitions, experimental conditions, and the number of replicates are as in Figure 2.

### The Effect of Oxygen in the Steady State

Oxygen had a pronounced effect on isoprene emission in light and in the dark. Overall, the rate of emission in the light was highest at 2% oxygen, and the rate decreased approximately 35% at higher oxygen concentrations and at 0% oxygen (Fig. 4A). The maximum dark-induced emission was also strongly reduced at 0% oxygen, more than 50% relative to 2% oxygen, but the maximum dark-induced emission rate was highest at 21% oxygen. The dark respiration rate increased with increasing oxygen concentration, although the change was small between 2% and 21% oxygen (Fig. 4A).

The substrate pools for both the postillumination and dark-induced isoprene emission decreased with increasing oxygen concentration from 2% to 21%, and the intermediate pools were further reduced by complete lack of oxygen (Fig. 4B). The rate of steady-state isoprene emission in the light matched the DMADP pool size well, but there was a mismatch between the maximum dark-induced isoprene emission and the dark pool size. In particular, the pool size was smaller at 21% oxygen, when the maximum emission rate was achieved, than under 2% oxygen, when the maximum emission rate was less (Fig. 4, compare A and B). This reflected the circumstance that the overall time period for the dark-induced process was shorter at higher oxygen concentration and was increasingly spread over time under lower oxygen concentration (for sample responses, see Fig. 5).

### Influence of Rapid Changes of Oxygen during the Dark Transient

In the following experiments, we asked whether the oxygen concentration influences only the preceding

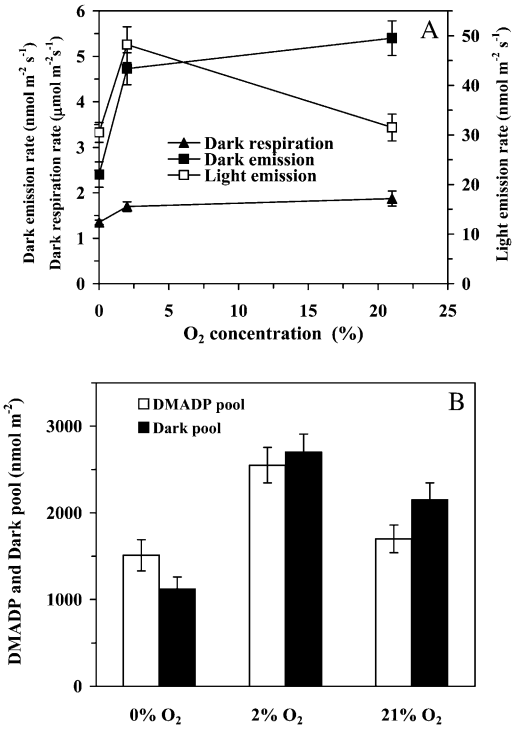


**Figure 4.** Comparison of the effects of oxygen on the steady-state isoprene emission in the light, on the maximum dark-induced emission rate, and on dark respiration rate (A), and the oxygen dependencies of the DMADP and dark pool sizes (B). Leaf temperature was maintained at 33°C and $CO_2$ concentration at 360 $\mu$mol mol$^{-1}$, and the quantum flux density was 600 $\mu$mol m$^{-2}$ s$^{-1}$ before the transient. Definitions of terms are as in Figure 2. Data are averages ± SD of at least four replicate experiments.

steady state in the light, and subsequent changes in the dark-induced emission are only an aftereffect, or whether oxygen concentration has a direct influence on isoprene emission in the dark. For this, we established the steady state under the standard atmospheric conditions but changed the gas composition simultaneously with darkening the leaf. Comparison of light/dark transients conducted under different oxygen concentrations indicated that changing oxygen concentration at the time of darkening had no detectable effect on the kinetics of postillumination isoprene release or on the DMADP pool size observed (Fig. 5). However, oxygen importantly modified the dark-induced emission. Complete lack of oxygen during the dark transient strongly suppressed dark-induced isoprene emission (Fig. 5, compare A and B). However, when a pulse of 2% oxygen of approximately 200 s was provided, dark-induced emission was significantly enhanced (Fig. 5C). Far-red light provided at the end of the dark-induced emission burst under normal oxygen did not change the emission pattern, but a small enhancement was observed in the experiment with a 2% oxygen pulse (Fig. 5, compare A and C). The observed effects were repeatable in all cases ($n$ = 3 replications).

### Temperature Dependencies in the Steady State

Both the steady-state emission rate in light and the maximum dark-induced emission rate were characterized by a curve with an optimum at around 40°C (Fig. 6A). Throughout the temperature response curve, the steady-state and dark-induced isoprene emission rates were strongly correlated (Fig. 6A, inset). The most pronounced difference between the light and dark processes was the complete cessation of the dark-induced emission at 20°C and below, while the light emission was still well detectable at the rates of 3 to 6 nmol m$^{-2}$ s$^{-1}$. This cessation of the dark-induced emission at low temperatures was also responsible for a positive $x$ intercept in the relationship of maximum dark-induced versus light emission rate (Fig. 6A, inset).

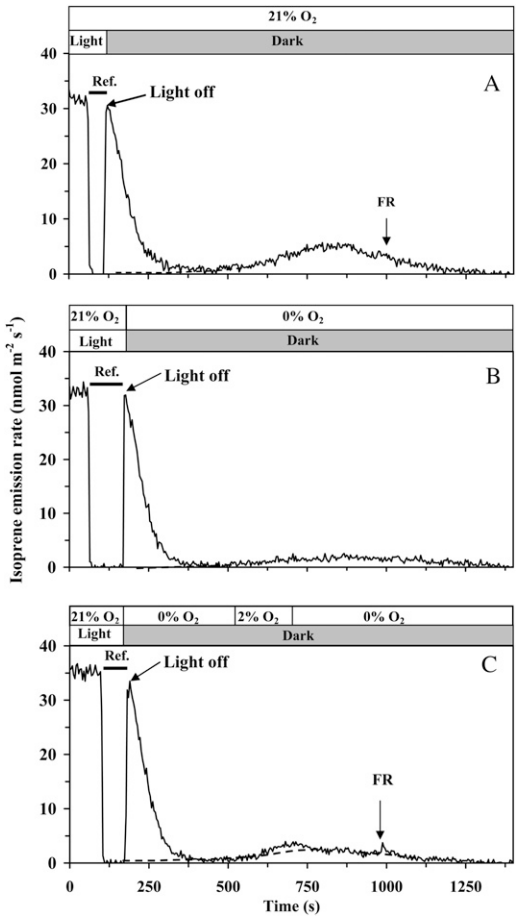


**Figure 5.** Comparison of the effects of oxygen concentration and far-red light (FR) during light/dark transients on the dark-decay kinetics of isoprene emission. In A, the whole postillumination process was measured under 21% oxygen. In B and C, oxygen concentration was changed to 0% simultaneously with switching off the light. In B, oxygen concentration was maintained at this level until the end of the transient, while in C, oxygen concentration was temporarily raised to 2% between 600 and 700 s. In all cases, quantum flux density prior to darkening was 600 $\mu$mol m$^{-2}$ s$^{-1}$, and $CO_2$ concentration was maintained at 360 $\mu$mol mol$^{-1}$ throughout the experiment. Horizontal bars denote the periods when the measurement system was switched to the reference line.

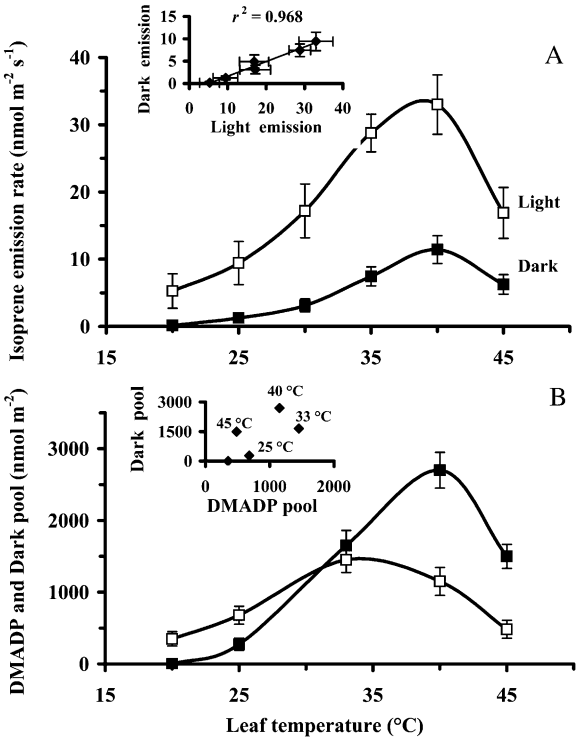


**Figure 6.** Temperature dependencies of the steady-state isoprene emission rate in the light and the following maximum rate of dark-induced emission (A) as well as the corresponding DMADP and dark pool sizes (B). The inset in A demonstrates the correlation between the steady-state emission rate in light and the maximum dark-induced emission rate measured under different temperatures, while the inset in B shows the corresponding relationship between the dark pool and the DMADP pool. At least four replicate experiments were conducted, and the error bars correspond to SD. The definitions of terms are as in Figure 2. Ambient $CO_2$ concentration was maintained at 360 $\mu$mol mol$^{-1}$, oxygen concentration at 21%, and quantum flux density was 600 $\mu$mol m$^{-2}$ s$^{-1}$ prior to darkening.

Stronger reduction of the dark-induced isoprene emission also resulted in a greater $Q_{10}$ value (i.e. increase in the process rate produced by raising temperature by 10°C) of 4.9 over the increasing temperature range of 25°C to 35°C than in the case of steady-state emission in the light ($Q_{10}$ = 2.9).

DMADP pool size changed in parallel with the steady-state emission rate at temperatures up to approximately 35°C (Fig. 6, compare A and B). At higher temperatures, DMADP pool size started to decrease while the emission rate still increased (Fig. 6). In contrast, the dark pool size and the maximum dark-induced isoprene emission rate changed in parallel throughout the entire temperature response curve (Fig. 6). DMADP and dark pool size were correlated at temperatures below 35°C, but at higher temperatures, the dark pool was much higher than the DMADP pool, being approximately 2-fold larger than the DMADP pool at 40°C and more than 3-fold larger at 45°C (Fig. 6B).

The onset of the dark-induced emission accelerated at higher temperatures, and the peak rate occurred earlier. For example, at 33°C, the peak of the dark-induced emission arrived at 7 to 9 min after darkening, but at 44°C, this time interval shortened to 4 min. Due to faster induction at higher temperatures, the dark-induced process ran partly into the postillumination isoprene emission. Nevertheless, the two processes could be satisfactorily separated by determining the baseline for the first process by extrapolation, as detailed in "Materials and Methods."

### Application of Fosmidomycin

Application of a 20 $\mu$M solution of fosmidomycin, a known inhibitor of the second enzyme of the MEP pathway, 1-deoxy-D-xylulose-5-phosphate reductoisomerase (DXR), inhibited the steady-state isoprene emission rate by 93% to 95% after 20 min from the application (Fig. 7, A and B). At this state, the photosynthetic $CO_2$ assimilation rate and quantum yield of PSII did not change significantly, while stomatal conductance even slightly increased (data not shown). The maximum dark-induced emission rate also decreased in response to fosmidomycin, but only by about half (Fig. 7B). Despite the significant inhibition of the emission rate, the isoprene synthase rate constant was not affected by the fosmidomycin treatment (Fig. 7B).

After light was turned off in the inhibited state, the postillumination (DMADP) pool was very small, about 4% to 6% of the uninhibited control (Fig. 7, A and C). However, the duration of the dark-induced isoprene emission process had increased, so that the integral pool was smaller only by about 20% to 25% than in the control (Fig. 7, A and C; e.g. the dark pool size was 2,120 nmol m$^{-2}$ prior to fosmidomycin feeding and 1,680 nmol m$^{-2}$ after feeding in the experiment in Fig. 7A). Short light pulses given during the dark-induced emission did not induce additional emission of isoprene, contrary to the uninhibited state (compare Fig. 1 with Fig. 7A).

## DISCUSSION

### Characteristics of Dark-Induced Isoprene Emission vis-a-vis Steady-State Emission in Light

The responses of steady-state emission of isoprene observed in our study, increase of the emission with increasing quantum flux density (Fig. 2), emission maximum close to the $CO_2$ compensation point (Fig. 3), increase of emissions at 2% oxygen relative to 21% (Fig. 4A), and emission maximum at a leaf temperature of approximately 40°C (Fig. 6A), and control of these changes in isoprene emission rate by DMADP pool size and isoprene synthase rate constant confirm our previous observations in aspen (Rasulov et al., 2009b, 2010). The emissions during light rely on a chloroplastic DMADP pool synthesized in the light

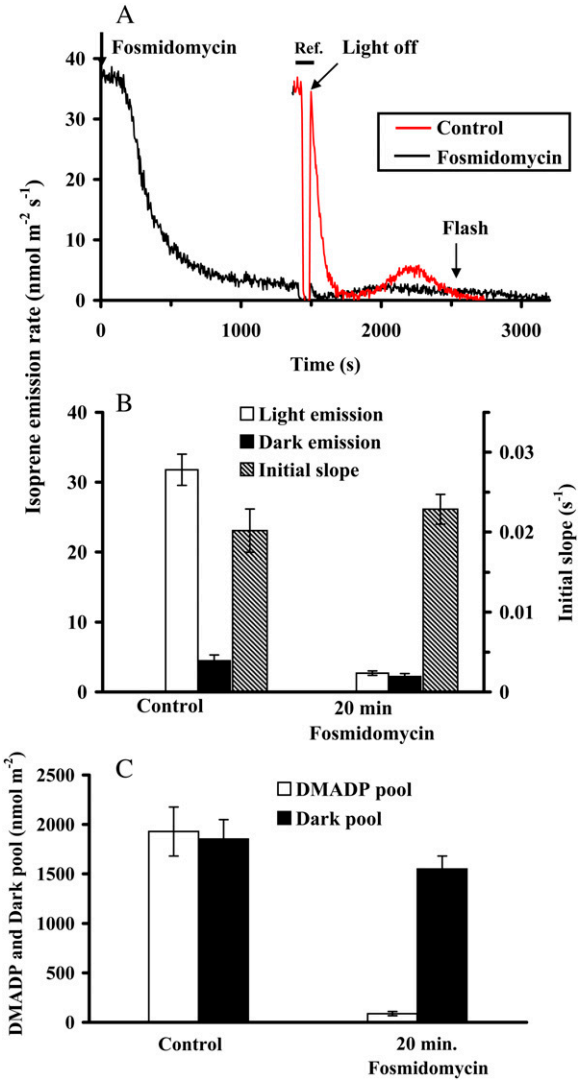


**Figure 7.** A sample response of the kinetics of the fosmidomycin effect on isoprene emission (black line) and comparison with the kinetics of isoprene release without fosmidomycin (red line; A), the influence of fosmidomycin on the steady-state isoprene emission in the light and on the maximum dark-induced isoprene emission, as well as the rate constant of isoprene synthase (B), and on the corresponding DMADP and dark pool sizes (C). In A, both the experiments without and with fosmidomycin were conducted with the same leaf. The experiment without fosmidomycin was conducted first, and after the leaf had reached the steady state again following the transient (20–30 min after switching on the light again), 20 $\mu$M aqueous solution of fosmidomycin was applied (time 0) and the reduction of isoprene emission was monitored in light until an apparent steady state was reached. At 1,350 to 1,450 s, the reference line was measured (Ref.; horizontal bar), and at 1,450 s, the light/dark transient was carried out according to the standard protocol (Fig. 1). A 2-s pulse of light (600 $\mu$mol $m^{-2}$ $s^{-1}$) was given at 2,550 s. To facilitate visual examination of the patterns, the transient without fosmidomycin was overlaid to the fosmidomycin experiment such that the moment of leaf darkening was exactly synchronized in both experiments. In this experiment, the dark pool size was 2,120 nmol $m^{-2}$ prior to fosmidomycin feeding (red line) and 1,680 nmol $m^{-2}$ after feeding (black line). In B and C, data are averages ± SD of four replicate experiments. All environmental conditions are as in Figure 2.

(with some contribution of IDP) that, after stopping the light, can support postillumination isoprene release for 200 to 300 s (Fig. 1). In contrast, dark-induced isoprene emission is elicited after this DMADP pool is depleted. Different time kinetics of the postillumination and dark-induced isoprene emission suggest a different mechanism of origin of these two processes. However, so far, only a single enzyme is known to be responsible for isoprene production in plants, the isoprene synthase, located in chloroplasts, that uses DMADP as the substrate (Silver and Fall, 1995; Vickers et al., 2010), suggesting that the dark-induced isoprene release must come from chloroplasts. In fact, studies in transgenic plants demonstrate that isoprene synthase is not functionally active in cytosol (Vickers et al., 2011).

Measurements of isoprene synthase rate constants at different times during the dark/light transition (Fig. 1; Li et al., 2011) indicated that isoprene synthase activity is not altered in darkness, at least during the period of the transient. Thus, the problem of understanding the nature of dark-induced isoprene emission reduces to understanding the origin of the substrate DMADP in the dark. In the light, DMADP is synthesized via the chloroplastic MEP pathway, which requires pyruvate and glyceraldehyde phosphate (GAP) as precursors and photosynthetically produced ATP (CTP) and NADPH as energetic cofactors. In the dark, photosynthesis is absent; therefore, either another pathway for the synthesis of DMADP or at least another pathway for the synthesis of the energetic cofactors is required. Our experiments showed a strong dependence of dark-induced isoprene emission on environmental conditions preceding leaf darkening, confirming the strong temperature dependence (Fig. 6; Li et al., 2011) and further highlighting major light (Fig. 2), $CO_2$ (Fig. 3), and oxygen (Fig. 4) dependencies. Similar regulation and strong correlations between steady-state isoprene emission and maximum dark isoprene emission observed through the environmental dependencies (Figs. 2–6) suggest that dark-induced emission is at least partly determined by carbon metabolites formed in light.

### Can Cytosolic Precursors of Isoprene Be Responsible for the Emissions in the Dark?

The key question in understanding the dark induction of isoprene release is what carbon and energy sources are responsible for isoprene formation in the dark. First, one may hypothesize that in the dark, DMADP can be formed from IDP by isopentenyl diphosphate isomerase. It is known that in cytosol, IDP, and DMADP in equilibrium with it, is formed in large quantities via the mevalonate pathway that functions independently of the chloroplastic MEP pathway (Disch et al., 1998; Lichtenthaler, 1999). Cytosolic DMADP is not readily transported to chloroplast, but it is still possible that IDP can be transported from the cytosol into the chloroplast (Rodríguez-Concepción and Boronat, 2002; Hemmerlin et al., 2003). This transport was more active under conditions of suppressed

MEP metabolism (e.g. in etiolated leaves, where the imported IDP can be used to support synthesis of the components of the photosynthetic machinery; Rodríguez-Concepción et al., 2004). However, direct measurements have shown very limited rates of IDP transport into chloroplasts in adult leaves under normal circumstances (Lichtenthaler, 1999; Hemmerlin et al., 2003; Dudareva et al., 2005). Even if very high nonphysiological exogenous concentrations of IDP and DMADP were used, the cytosolic contribution to the chloroplastic IDP and DMADP pool was only 1% to 2% (Disch et al., 1998; Eisenreich et al., 2001). In addition, the transmembrane carrier of IDP has also not yet been found (Flügge and Gao, 2005). In the most conclusive experiments with $^{13}C$ labeling, it has been shown that when the chloroplastic MEP pathway was blocked by fosmidomycin, $^{13}C$-labeled IDP and DMADP from the mevalonate pathway were not incorporated into the remaining slow isoprene emission (Affek, 2003; Affek and Yakir, 2003). In fact, there is evidence suggesting the opposite transport. During active isoprenoid synthesis in cytosol (e.g. during intensive synthesis of sterols), when $C_5$ building blocks are transported from chloroplast to the cytosol (Lichtenthaler, 2007).

Our kinetics results also do not support the mevalonate pathway origin of isoprene in the dark. The cytosolic DMADP pool and corresponding IDP pool in equilibrium with it exceed the corresponding chloroplastic pools by about an order of magnitude (Falbel and Sharkey, 2005; Rasulov et al., 2009a; Ghirardo et al., 2011). Given these huge pools, isoprene emission could continue in the presence of a dark-induced transport of IDP from cytosol to chloroplast for hours. Yet, the dark-induced isoprene emission decays within 20 to 25 min after induction, suggesting an intermediate pool (dark pool) size comparable to the chloroplastic DMADP pool size (i.e. a relatively small pool compared with the cytosolic DMADP/IDP pool).

Collectively, the experimental evidence observed in our study, tightly related rates and pool sizes of the light- and dark-induced emissions throughout the range of light as well as ambient $CO_2$ and oxygen concentrations (Figs. 2–5), is not in line with the cytosolic origin of the substrate for the dark-induced isoprene emission. The cytosolic pools are much too large to be regulated that fast, and there is also no known mechanism leading to such environmental dependencies of cytosolic pools. Also, the literature evidence about the interactions between the cytosolic mevalonate and chloroplastic MEP pathways for isoprenoid synthesis has so far shown only a minor contribution of cytosolic IDP and DMADP to chloroplastic isoprenoid synthesis.

### The MEP Pathway Is Temporarily Reactivated in the Dark

The previous discussion suggests that the DMADP for dark-induced isoprene emission is de novo synthesized in the chloroplast. Strong correlations between the steady-state emission in light and the dark-induced emission and corresponding pool sizes through the light and $CO_2$ dependencies of isoprene emission (Figs. 2 and 3) further suggest that the total amount of isoprene emitted in the dark is determined by some chloroplastic precursor pools, converted into DMADP after the cessation of postilluminatory isoprene release. After darkening, the rate of the postillumination isoprene emission starts to decrease immediately, indicating that de novo formation of DMADP by NADPH-dependent conversion of 4-hydroxy-3-methyl-2-(*E*)-butenyl-diphosphate (HMBDP) is blocked and the postillumination isoprene emission is proceeding at the expense of preaccumulated DMADP (Fig. 8; Rasulov et al., 2009a). On the basis of existing evidence (Rohdich et al., 1999; Zepeck et al., 2005), it is very likely that other reactions of the MEP pathway supported by photosynthetically generated NADPH (DXR, HMBDP synthase [HDS], and HMBDP reductase [HDR]) and ATP and CTP (CDP-methyl-D-erythritol kinase and CDP-methyl-D-erythritol synthase, Fig. 8) also stop as soon as the light is turned off. Although the flux through the pathway ceases, the intermediate pools remain present at least for some time in the dark. The size of these pools is probably greater in conditions where the flux through the pathway has been higher prior to the darkening. This suggestion is in line with the observed parallel trends between the dark-induced emission pool and the preceding steady-state isoprene emission rate in the light. This evidence collectively supports our conclusion that the precursors of the dark-induced isoprene emission are the ATP- and NADPH-dependent intermediate pools of the MEP pathway, "frozen" as a result of the absence of the energetic cofactors.

The reliance of isoprene emission on the light-dependent synthesis of ATP and NADPH was shown already in the very early experiments by Sanadze and colleagues (Sanadze, 1966; Mgalobilishvili et al., 1978; Sanadze and Baazov, 1985) and confirmed later (Loreto and Sharkey, 1990). In fact, isoprene emission from isolated chloroplasts in the dark was enhanced by exogenous ATP and NADPH (Sanadze, 1966), conclusively indicating that not only the light-dependent but also the dark-induced isoprene emission is supported by the energetic metabolites. This evidence suggests that the slow dark-induced maximum emission rate is limited by the availability of ATP and NADPH in the dark. On the other hand, exogenous ATP and NADPH did not affect the isoprene emission of isolated chloroplasts in the light, suggested to reflect the saturating level of these cofactors in photosynthesizing chloroplasts (Sanadze, 1966; Seemann et al., 2006). On the other hand, it has been discovered that the two Fe-S-containing enzymes in the pathway, immediately prior to IDP and DMADP formation, HDS and HDR (Fig. 8), can directly accept electrons from ferredoxin in light and switch to NADPH in darkness (Seemann et al., 2006; Seemann and Rohmer, 2007).

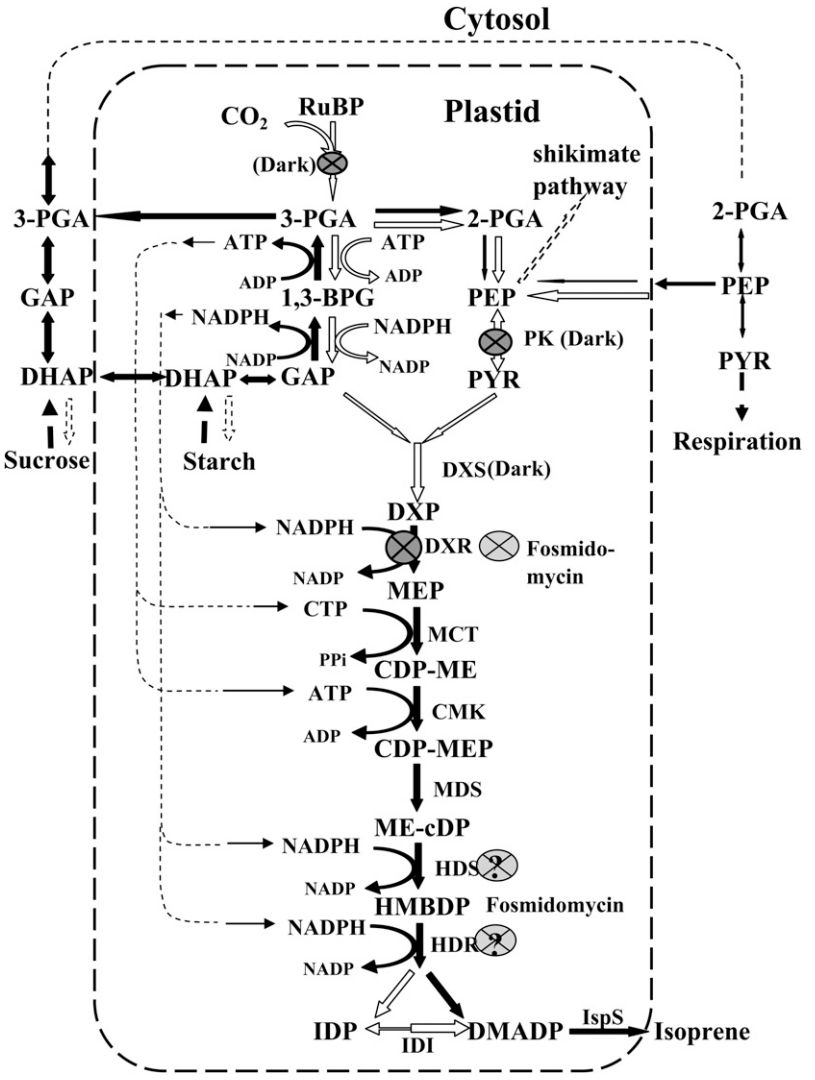


**Figure 8.** Schematic representation of the chloroplastic MEP pathway and likely interactions with the cytosolic processes. Enzymatic steps expected to be most susceptible to darkness are indicated by black arrows. The steps inhibited in darkness are denoted by dark gray circled crosses, while the known control point of fosmidomycin inhibition, DXP reductoisomerase (Kuzuyama et al., 1998), is denoted by a light gray circled cross. Additional steps presumably inhibited by fosmidomycin are shown by light gray circled question marks. Abbreviations are as follows: RuBP, ribulose-1,5-bisphosphate; 3-PGA, 3-phosphoglycerate; 2-PGA, 2-phosphoglycerate; 1,3-BPG,1,3-bisphosphoglycerate; GAP, glyceraldehyde 3-phosphate; DHAP, dihydroxyacetone phosphate; PEP, phospho*enol*pyruvate; PYR, pyruvate; DXP, 1-deoxy-D-xylulose-5-phosphate; MEP, 2-*C*-methyl-D-erythritol-4-phosphate; CDP-ME, 4-(cytidine-5-diphospho)-2-*C*-methyl-D-erythritol; CDP-MEP, 2-phospho-4-(cytidine-5-diphospho)-2-*C*-methyl-D-erythritol; ME-cDP, 2-*C*-methyl-D-erythritol 2,4-cyclo-diphosphate; HMBDP, 4-hydroxy-3-methyl-2-(*E*)-butenyl-diphosphate; IDP, isopentenyl diphosphate; DMADP, dimethylallyldiphosphate; DXS, DXP synthase; DXR, DXP reductoisomerase; MCT, CDP-methyl-D-erythritol synthase; CMK, CDP-methyl-D-erythritol kinase; MDS, methyl-D-erythritol-CDP synthase; HDS, HMBDP synthase; HDR, HMBDP reductase; IDI, IDP isomerase; IspS, isoprene synthase; PK, pyruvate kinase.

Fast dark inactivation of DXR (Loivamäki et al., 2007) may also indicate that carbon input into the MEP pathway is rapidly stopped (Fig. 8). However, the observation in our study that short light pulses given during the initial increasing phase of the dark-induced emission cause immediate activation of emission, as additional DMADP can be rapidly produced at the expense of ATP and NADPH formed by photosynthetic electron transport, still supports the energetic limitation of the process in the presence of sufficient carbon in the pathway (Fig. 1A). The fact that these same light pulses result in no additional isoprene release during the decay phase of the dark-induced emission (Fig. 1B) indicates that the decline of the dark-induced emission results from depletion of the carbon pool present in the MEP pathway. On the basis of these experimental findings, we suggest that the increasing phase of the dark-induced isoprene emission is rate limited by the availability of energetic cofactors needed to convert the existing intermediates of the MEP pathway into DMADP, but input of additional carbon into the pathway is blocked in the dark as well. In fact, this result is in accordance with the data demonstrating that chloroplastic pyruvate kinase, the input enzyme of the MEP pathway catalyzing the formation of pyruvate from phospho*enol*pyruvate (Andre et al., 2007), is rapidly inactivated in the dark (Fig. 8; Chastain et al., 2002, 2008). Thus, the total amount of isoprene emitted in the dark (postillumination and dark induced) indicates the total amount of carbon in the MEP pathway. This idea is supported by data showing that the intermediates of the MEP pathway, 1-deoxy-D-xylulose-5-phosphate (DXP) and CDP-methyl-D-erythritol (Cassera et al., 2007), as well as 2-*C*-methyl-D-erythritol 2,4-cyclodiphosphate (Rivasseau et al., 2009), do accumulate in plant tissues, constituting the reserve pools for further synthesis of isoprenoids under stress conditions (Ostrovsky et al., 1994; Hwang and Sakakibara, 2006).

Coordinated changes in steady-state and dark-induced emission responses (Fig. 6A) further underscore that both emissions rely on a similar carbon source. However, the dark pool size was significantly

larger at higher temperatures than the DMADP pool (Fig. 6B). Multiple enzymatic steps are needed to convert MEP into DMADP, and each of these can have a slightly different temperature dependence of maximum activity as well as differences in the temperature dependence of $K_m$ values for the reaction substrates and cofactors. Such differences in temperature-dependent regulation can be responsible for the accumulation of the dark pool under higher temperatures and depletion under lower temperatures. Analogously, partial steps of photosynthesis and glycolysis are known to be regulated differently by temperature, resulting in accumulation and depletion of certain photosynthetic intermediate pools (Pastenes and Horton, 1996) and in oscillations in glycolysis intermediates (Mair et al., 2005) under different temperatures.

### Chloroplastic Glycolysis as a Candidate Source of Energy for Dark-Induced Emission

The pools of NADPH and ATP (plus thylakoid proton gradient) are sufficient to support photosynthetic $CO_2$ fixation only for a few seconds in the dark (Pearcy et al., 1997). Cessation of photosynthetic $CO_2$ uptake implies that the ATP pool rapidly drops to the level completely stopping ribulose-1,5-bisphosphate regeneration via the ribulose-5-phosphate kinase reaction in the pentose phosphate carbon reduction cycle. Thus, the light-generated ATP and NADPH pools are depleted so fast that they cannot significantly participate in either the postillumination isoprene emission or the dark-induced isoprene emission. Nevertheless, after a sustained dark period, significant levels of ATP and NADPH have been detected in intact chloroplasts and in chloroplasts nonaqueously extracted from leaves (Inoue et al., 1978; Hampp et al., 1982; Gerst et al., 1994; Cruz et al., 2008). The observation that isoprene emission drops close to zero after the postillumination process has completed, but then increases again, passing through a maximum after about 600 s, is in line with the understanding that the levels of energetic metabolites do drop rapidly after darkening but slowly increase again in the dark (Loreto and Sharkey, 1993; Laisk and Oja, 1998). This evidence collectively suggests the activation of certain metabolic processes in darkness that can provide energetic and reductive equivalents for the dark-induced isoprene release. In particular, dark activation of chloroplastic glycolysis (Inoue et al., 1978; Hoppe et al., 1993; Eastmond and Rawsthorne, 2000; Baud et al., 2007) and chlororespiration (Bennoun, 1982, 2001; Nixon, 2000) are the candidate processes explaining the dark emission.

Glycolysis, either in the cytosol or in the chloroplasts, has been shown to be a potential source of carbon skeletons for isoprene biosynthesis if photosynthesis is inactive (Loreto et al., 2000). The capacity of isolated chloroplasts to form the intermediates of glycolytic pathway such as phospho*enol*pyruvate has been known for a long time (Yamada and Nakamura, 1975). Although the rate of chloroplastic glycolysis is slower than the rate of cytosolic glycolysis, it can be sufficient to support not only the biosynthesis of lipids, amino acids, and proteins (Ramachandra and Das, 1987; Hoppe et al., 1993) but the MEP pathway of isoprene synthesis as well. It has been suggested that plastids lack some of the key enzymes of glycolysis, such as enolase and phosphoglycerate mutase (Givan, 1999), implying an obligatory cytosolic step for isoprene synthesis (Fig. 8). However, these enzymes have been found to be active in heterotrophic plastids (Muñoz-Bertomeu et al., 2009; Andriotis et al., 2010) and recently also were demonstrated to be present in chloroplasts (Joyard et al., 2010; Bayer et al., 2011). Nevertheless, in the dark, the terminal part of the glycolytic pathway converting 3-phosphoglycerate (3-PGA) to phospho*enol*pyruvate and pyruvate (including phosphoglyceromutase and enolase) is not active in the chloroplasts (Stitt and ap Rees, 1979; Bagge and Larsson, 1986; Andriotis et al., 2010), but the $PGA^{2-}$ form is translocated from the chloroplast into the cytosol in exchange of phosphate (Flügge and Heldt, 1984), and the pathway is completed there. Serious disturbances of metabolism were observed in leaves with genetically decreased activity of cytosolic enolase (Voll et al., 2009), indicating the functional importance of the integration of cytosolic and chloroplastic glycolytic pathways in the dark.

As for the input of the glycolytic pathway, after darkening, the triosephosphates GAP and dihydroxyacetone phosphate are immediately available for GAP dehydrogenase/PGA kinase reactions. In a longer term, starch may be hydrolyzed via the reversible phosphorylase pathway, followed by the oxidative pentose phosphate cycle (Kaiser and Bassham, 1979a; Stitt and Heldt, 1981; Stitt et al., 1985; Troncoso-Ponce et al., 2009). It has been experimentally verified that in chloroplasts, 3-GAP is oxidized to 3-PGA in the dark, with simultaneous formation of ATP and reducing power in the form of NADPH and reduced ferredoxin ($Fd^-$; Fig. 8; Kow et al., 1982). For stable ATP production by this pathway, NADPH (or $Fd^-$) must be oxidized to ensure the presence of the electron acceptor $NADP^+$ (or Fd). The chlororespiratory pathway has sufficient potential to oxidize NADPH (Bennoun, 2001; Peltier and Cournac, 2002). In addition, the Mehler reaction of oxygen reduction is an efficient electron acceptor from $Fd^-$ (Kow et al., 1982; Ji et al., 1992; Tuttle et al., 2007). In the oxygen-free atmosphere, the formation of PGA from GAP and ATP from ADP is practically stopped, indicating the strictly rate-limiting deficit of the electron acceptor NADP+ (Kow et al., 1982; Tuttle et al., 2007). Thus, the need for both the reducing power and ATP by the MEP pathway creates ideally suitable conditions for cooperation between the glycolytic and MEP pathways in the dark. Overall, the major reduction of dark-induced isoprene emission by low oxygen and the rapid increase of emission after a pulse of oxygen in darkened leaves (Figs. 4 and 5) are in accordance with the tight coupling of dark emissions with ATP and NADPH availability.

The strong positive effect of oxygen on the dark-induced isoprene emission (Figs. 4 and 5) supports the combined participation of oxidizing agents in the process as increased oxidation of $Fd^-$ and NADPH supports faster ATP formation, but oxygen is not the only sink of the reducing power. Interestingly, pulses of far-red light, known to stimulate the emission of isoprene in light (Loreto and Sharkey, 1990), slightly stimulated the dark-induced emission in the absence of oxygen (Fig. 5C) but had no or very little effect in the presence of oxygen (Fig. 5A). This suggests that cyclic photophosphorylation helps to generate some ATP under these conditions, but one should not forget that far-red light excites PSII as well (Laisk et al., 2010). The positive effect of oxygen on isoprene emission due to its role as an electron acceptor may be even stronger than the observed enhancement of emissions, because some enzymes of the MEP pathway (HDS and HDR) are inactivated by oxygen, at least in vitro (Ogrel et al., 1996). If this happens also in intact leaves, then the positive effect of oxygen on ATP synthesis must overrun its inhibitory effect on the enzymes, or in vivo, HDS and HDR are protected from being inactivated by oxygen (Adam et al., 2002).

The delayed activation of the dark isoprene emission needs an explanation. During photosynthesis, triosephosphates are available, facilitating the immediate reversal of the GAP dehydrogenase/PGA kinase complex toward ATP and NADPH synthesis as soon as light is turned off. However, during photosynthesis, the complex is driven toward the anabolic direction not only by photosynthetically supported high ATP/ADP and NADPH/$NADP^+$ ratios but by the high PGA/GAP ratio as well (Heber et al., 1986; Gerst et al., 1994). The PGA/GAP ratio rapidly increases after darkening due to the postillumination conversion of ribulose-1,5-bisphosphate into PGA and the consumption of trioses in carbohydrate synthesis (Laisk et al., 1984; Loreto and Sharkey, 1993). The catabolic ATP and NADPH synthesis can begin only after the chloroplastic PGA pool decreases in the dark. This pool is first equilibrated with the cytosolic PGA pool via the phosphate translocator, and the total PGA pool is slowly consumed by mitochondrial respiration. The latter process requires about 3 to 6 min (Kaiser and Bassham, 1979b; Loreto and Sharkey, 1993). We suggest that the triggering mechanism of the dark ATP synthesis is the postillumination reduction of PGA level: the flux through the glycolytic pathway activates only after the large photosynthetically generated PGA pool is consumed. As the mitochondrial respiration rate is strongly increasing with increasing temperature, faster induction of dark isoprene emission, as observed in our study and by Li et al. (2011), can be explained by faster depletion of the PGA pool. Analogously, a stronger oxygen effect on dark-induced isoprene emission than on steady-state isoprene emission can be explained by oxygen-amplified dark respiration rate (Fig. 4A).

**Further Evidence from Fosmidomycin Treatment: Fosmidomycin Likely Inhibits at Least One More Step**

Fosmidomycin is known to inhibit the second enzyme of the MEP pathway, DXR (Kuzuyama et al., 1998; Zeidler et al., 1998; Schwender et al., 1999). Treatment of leaves with this inhibitor resulted in the inhibition of steady-state isoprene emission by approximately 95% within 20 min after application (Fig. 7, A and B). Fosmidomycin also reduced the DMADP pool size responsible for isoprene emission in light by a similar percentage (Fig. 7C), while the rate constant of isoprene synthase was maintained (Fig. 7B). In contrast, the dark pool responsible for the dark-induced emission decreased only by 25% to 28% compared with the control (Fig. 7C), although the maximum dark-induced emission rate was twice slower than in the uninhibited control (Fig. 7B) and was spread over a longer time period of 25 to 30 min (Fig. 7A). At first glance, this result speaks against the hypothesis that the integral of the dark-induced emission is determined by the total pool of the MEP pathway. If the first reaction of the MEP pathway is inhibited, all the intermediates are expected to be converted to DMADP, and by the time of darkening, all the intermediates of the MEP pathway should have been depleted (Fig. 8). On the basis of available knowledge, only metabolites upstream of DXR, such as DXP, could build up, provided that accumulation of DXP is not affecting the rate of its own synthesis and the processes further upstream (Fig. 8). Thus, slow conversion of DXP by DXR to MEP under fosmidomycin inhibition can provide the explanation for the dark-induced emission of isoprene and suggests that DXP is the main component of the dark pool.

The difficulty with the DXP accumulation hypothesis is that it takes 30 to 40 min after fosmidomycin application for maximum inhibition (Fig. 7A). Provided that DXP synthesis is not altered, a huge pool is accumulating that could sustain dark-induced isoprene emission for far longer than was observed. In fact, there is an alternative possibility for the maintenance of a significant pool of MEP pathway intermediates responsible for dark-induced isoprene emission in fosmidomycin-inhibited leaves. Such a maintenance of the intermediate pool is possible if fosmidomycin partly inhibited another more terminal step in the pathway, allowing the section of the pathway between the two inhibited enzymes to partly retain the previous pool size. Such a candidate enzyme is HMBDP synthase or HMBDP reductase (Fig. 8), which under normal circumstances do not constrain the flux through the MEP pathway (Flores-Pérez et al., 2008). In fact, an analysis of the intermediates of the MEP pathway after application of fosmidomycin demonstrated that the level of MEP is decreased only by 15% to 17%, the level of CDP-methyl-D-erythritol and CDP-MEP by 30%, and the level of 2-C-methyl-D-erythritol 2,4-cyclo-diphosphate by 40% (Cassera et al., 2007); that is, practically stopping the pathway by turning off the initial reaction was not accompanied by depletion

of the key intermediates before DMADP. Possible inhibition of the MEP pathway at two different points is in accordance with the observed dark-induced isoprene release in fosmidomycin-inhibited leaves. In addition to our observation, other data also lend indirect support to the hypothesis that fosmidomycin is not as selective an inhibitor of DXR as assumed before (Barta and Loreto, 2006). We conclude that more work is needed to test the specificity of fosmidomycin as the inhibitor of the MEP pathway.

### A Model of Dark-Induced Isoprene Emission

On the basis of the aforementioned evidence, we suggest the following mechanism for the dark-induced isoprene emission. In light prior to darkening, the chloroplastic MEP pathway adjusts its rate and intermediate pool sizes dependent on the environmental conditions, as described earlier (Rasulov et al., 2009a, 2009b, 2010; Li et al., 2011). After darkening, photosynthetically supported ATP/ADP and NADPH/$NADP^+$ ratios rapidly drop, blocking the flux through the pathway but leaving intermediate pools of the MEP pathway more or less unchanged (rearrangements according to equilibrium conditions cannot be excluded). During the first minutes of darkness, the postillumination PGA pool is metabolized and the PGA kinase/GAP dehydrogenase complex activity shifts toward the catabolic direction, beginning to form ATP and NADPH (Fig. 8). The increasing availability of these energetic metabolites activates the MEP pathway again, resulting in isoprene emission in the dark, although with a slower rate than in the light. However, in the dark, the further input of carbon skeletons into the pathway is blocked due to the dropping level of pyruvate in the chloroplast and the inactivation of the enzyme(s) DXS or DXR (Fig. 8), feeding the MEP pathway with carbon intermediates. As a result of the lack of further carbon input into the pathway, the dark-induced isoprene emission decreases and ceases again after the pools of the MEP pathway are exhausted (Fig. 8). According to this model, the total amount of isoprene emitted in the dark characterizes the total pool size of the MEP pathway. Alternatively (or additionally), the low level of GAP in the absence of photosynthesis may limit the glycolytic production of energetic cofactors.

## CONCLUSION

The kinetic evidence suggests that the observed emission of isoprene in the dark is the continuation of the photosynthetically supported pathway, now energetically supported by ATP and NADPH produced by the reversal of the reductive part of the chloroplastic pentose phosphate carbon reduction cycle toward glycolysis. The total amount of isoprene emitted in the dark is likely driven by the size of the intermediate pools of the MEP pathway as determined by preceding light, $CO_2$, and oxygen concentrations and temperature.

## MATERIALS AND METHODS

### Plant Material and Growing Conditions

One-year-old plants of hybrid aspen (*Populus tremula* × *Populus tremuloides*) clone 200 (for the genotype, see Vahala et al., 2003) were grown in an AR-95 HIL climatic chamber (Percival CLF Plant Climatics) in 4-L plastic pots filled with a mixture of peat and sand (1:1) under an optimized supply of water and nutrients as described previously (Rasulov et al., 2009a, 2009b, 2010). The photoperiod with incident quantum flux density of 550 $\mu$mol $m^{-2}$ $s^{-1}$ was 14 h, day/night temperatures were 26°C/20°C, and relative humidity was kept at 60%. In all the experiments, we used fully developed leaves, 20 to 30 d after bud burst, exhibiting maximum photosynthesis and isoprene emission rates.

### Measurements of $CO_2$ and Water Vapor Exchange

An ultrafast response gas-exchange system with two identical gas lines was used for the measurements (Laisk et al., 2002). The system features a clip-on-type leaf chamber with 8.04-$cm^2$ cross-section area and 0.3-cm height, and the gas flow rate in the system is maintained at 0.5 mmol $s^{-1}$, resulting in a system half-time of approximately 0.15 s (Rasulov et al., 2010). Two identical gas lines allowed for rapid measurement of reference line and sample. While the leaf was connected to channel 1, analyzers connected to channel 2 recorded the reference (zero) line. The channels could be switched in less than 1 s, and as soon as the leaf chamber was connected to channel 2, the analyzers essentially immediately recorded the water vapor, $CO_2$, and isoprene exchange rates at the gas concentrations preadjusted in channel 2 (Laisk et al., 2002; Li et al., 2011). Such a setup is particularly advantageous for fast measurement of transient responses, avoiding delays in the detection of leaf signals due to the stabilization of gas concentrations.

Light was provided by a Schott KL 1500 light source with a heat-reflecting filter (Optical Coating Laboratory). The air was mixed from pure nitrogen, oxygen, and $CO_2$ using calibrated dynamic mixers and humidified to result in a water vapor pressure deficit of 1.7 kPa (Laisk et al., 2002). The $CO_2$ concentration was measured with an infrared gas analyzer (LI-6251; Li-Cor), and the water vapor pressure was measured with a micropsychrometer integrated in the gas system (Laisk et al., 2002). The temperature of the leaf chamber was stabilized by a water jacket. The heat exchange of the leaf was enhanced by gluing the upper leaf surface to the glass window of the leaf chamber water jacket, resulting in leaf temperatures within 0.5°C of the water jacket. Because aspen has essentially no stomata on the upper leaf side, the gas-exchange rate of the leaf was not affected by this procedure. In fact, less than 2% of isoprene emission occurs through the upper epidermis (Fall and Monson, 1992). To avoid water condensation during high-temperature measurements, the gas-exchange tubing was thermostatted at 50°C.

### Measurements of Chlorophyll Fluorescence

Chlorophyll fluorescence was measured simultaneously with $CO_2$ and water exchange by a PAM 101 fluorimeter (H. Walz). Another Schott KL 1500 white light source was used to provide saturated light pulses of 14,000 $\mu$mol $m^{-2}$ $s^{-1}$ for 2 s to measure either the dark-adapted ($F_m$) or light-adapted ($F_m'$) maximum fluorescence yield. For dark-adapted minimum fluorescence yield ($F_0$), a third Schott KL 1500 light source equipped with a 720-nm narrow-pass interference filter (Andover Corp.) was used to illuminate leaves with a weak far-red light of 50 $\mu$mol $m^{-2}$ $s^{-1}$. The PAM 101 fluorimeter was operated at a frequency of 1.6 kHz for darkened leaves and at 100 kHz for illuminated leaves and during saturated pulses. The dark-adapted quantum yield of PSII was calculated as $(F_m - F_0)/F_m$ and the light-adapted quantum yield as $(F_m' - F)/F_m'$, where $F$ is the steady-state fluorescence yield. Dark-adapted quantum yield was typically measured at least 20 min after darkening. In the case of quantum yield measurements during light/dark transients, PSII activity was often also measured 5 to 6 min after darkening; thus, true $F_m$ level was not necessarily reached in such cases. Therefore, this quantum yield is denoted as quantum yield in dark (i.e. quantum yield with some residual nonphotochemical quenching).

## Isoprene Measurements

A proton transfer reaction mass spectrometer (PTR-MS; high-sensitivity version; Ionicon Analytik) was used to measure isoprene concentration. The PTR-MS has a response time of approximately 0.1 s and a detection limit of approximately 10 pmol $mol^{-1}$ for isoprene (Lindinger et al., 1998; Hansel et al., 1999). A standard gas with 5.74 $\mu$mol $mol^{-1}$ isoprene in $N_2$ (Hills Scientific) was used for calibration of the PTR-MS.

## Standard Experimental Protocol for Isoprene, Net Assimilation, and Chlorophyll Fluorescence Measurements in Light and Darkness

Standard conditions used in these experiments previously shown to result in maximum isoprene emission rate in aspen (Rasulov et al., 2010) were leaf temperature of 33°C, saturating incident quantum flux density of 600 $\mu$mol $m^{-2}$ $s^{-1}$, ambient $CO_2$ concentration of 360 $\mu$mol $mol^{-1}$, and oxygen concentration of 21%. After leaf enclosure in the chamber, the standard environmental conditions were established and the leaf was maintained under these conditions until stomata opened and steady-state $CO_2$ and isoprene emission rates were established, typically 15 to 20 min after leaf enclosure. The steady-state values of isoprene emission, net assimilation rate, and chlorophyll fluorescence were thereafter recorded.

After measurement of the steady-state values, the reference lines for isoprene, $CO_2$, and water were obtained by switching between sample and reference lines with identical incoming air composition. After about 50 to 100 s, the leaf chamber was returned to the sample line again and the leaf was darkened simultaneously (for sample measurements, see Fig. 1). The kinetics of isoprene emission were thereafter monitored through an initial rapid decay period of approximately 200 to 400 s following switching off the light and through the emission burst activated in the darkness between approximately 300 and 1,500 s following darkening (Fig. 1).

## Measurement of Response Curves of Light- and Dark-Induced Isoprene Release and Experiments with Changed Oxygen and $CO_2$ Concentrations in Darkness

To measure the responses of isoprene light and dark emissions to quantum flux density, temperature, and $CO_2$ and oxygen concentration, after recording the full transient under standard conditions, light was switched on again and the leaf was kept under the standard conditions until the previous steady-state values were observed, typically for 10 to 20 min. Thereafter, a given driver was changed, steady-state values were established, and the whole postillumination procedure was repeated. After this, steady-state values were established under light again, the given environmental driver was changed to a new level, and the whole procedure was repeated.

In additional experiments, the steady-state values were measured always at standard conditions, but the postillumination process was conducted either at a different $CO_2$ or oxygen concentration. In this case, the gas composition was changed simultaneously with darkening. In further experiments, either oxygen or $CO_2$ was changed at different times during the postillumination measurements (for a sample response, see Fig. 5C). Finally, short pulses of white light or far-red light of 1 to 4 s were given in additional experiments to check the energetic status of the leaves, the responsiveness of isoprene emissions to light, and the possible accumulation of reduced electron carriers between PSI and PSII (Figs. 1 and 5).

## Determination of the DMADP and Dark Pool Sizes

The method of Rasulov et al. (2009a) with modifications of Rasulov et al. (2010) was used to measure the pool size of the immediate precursor pool responsible for isoprene emission during the steady state. This pool can in principle consist of the sum of DMADP, the primary isoprene precursor, and IDP that is in equilibrium with DMADP (Li et al., 2011). Previous studies have demonstrated very low chloroplastic IDP/DMADP ratios (Ramos-Valdivia et al., 1997; Page et al., 2004), suggesting that chloroplastic IDP isomerase must be active (Brüggemann and Schnitzler, 2002). Thus, we suggest that the immediate precursor pool responsible for isoprene emission mainly consists of DMADP ($S_{DAMDP}$). The size of this pool was determined by integrating the fast (up to 200–400 s after darkening) dark decay of isoprene release (Rasulov et al., 2009a, 2010):

$$S_{DMADP} = \int_{t_0}^{t_f} I(t)dt \quad (1)$$

where $I(t)$ is the isoprene emission rate at time $t$, $t_0$ is the time of leaf darkening, and $t_f$ is the time of cessation of this process. Because the ultrafast system was used and the reference line was directly measured, no correction for the system inertia was needed (Rasulov et al., 2010). As a dark-induced process of isoprene emission starts at about 300 to 400 s after darkening (Rasulov et al., 2010; Li et al., 2011), the baseline for integration was found by linearly extrapolating the isoprene emission rate over 400 to 600 s after darkening (rising part of the dark-induced isoprene emission) to zero level (Fig. 1), as described by Rasulov et al. (2010) and Li et al. (2011). For the experiments with short pulses of white light given during the dark decay period, we assumed that the isoprene emission relies on the DMADP synthesized during the light pulse, and again, $S_{DAMDP}$ was determined using the same extrapolated baseline (Fig. 1A; measurements between 500 and 600 s since the start of the recording).

In the case of the metabolite pool responsible for the secondary increase of isoprene emission, defined as the "dark" pool ($S_{dark}$) here and the "early metabolite pool of the MEP pathway" by Li et al. (2011), we employed an analogous procedure, by integrating the emission rate over the induced emission burst and employing the baseline established previously for the determination of DMADP pool size (for sample relationships, see Fig. 1).

## The Rate Constant of Isoprene Synthase

The rate constant of isoprene synthase, $k_a$ ($s^{-1}$), was calculated from the early dark-decay data of isoprene emission as described by Rasulov et al. (2010). In short, $k_a$ is the slope of isoprene emission rate, $I$, versus the $S_{DMADP}$ relationship measured throughout the rapid dark decay. This relationship was established by determining the paired $S_{DMADP}$ and $I(t)$ values at any time during the dark decay. At time $t_1$, the DMADP pool size corresponding to $I(t_1)$ is given as

$$S_{DMADP}(t_1) = \int_{t_1}^{t_d} I(t)dt \quad (2)$$

where $t_d$ is the time for the depletion of the DMADP pool; thus, paired values of $S_{DMADP}(t)$ and $I(t_1)$ were derived. Overall, the relationship was linear, reflecting the very large $K_m$ value of isoprene synthase for DMADP (Rasulov et al., 2009a).

## Application of Fosmidomycin

Fosmidomycin (Invitrogen), a known inhibitor of the MEP pathway (Kuzuyama et al., 1998; Zeidler et al., 1998; Schwender et al., 1999), was fed to the leaves through the petiole at 20 $\mu$M aqueous solution as described by Rasulov et al. (2009a). In the light, isoprene emission usually decayed by about 95% within 20 to 30 min from the application of the fosmidomycin. After reaching this low value, postillumination isoprene emission measurements were carried out using the standard protocol (for a sample response, see Fig. 7A).

## Data Analyses

In all cases, four to 10 replicate experiments were carried out, and reported data area means ± SD. Whenever pertinent, means were compared by ANOVA and considered significantly different at $P < 0.05$.

Received March 11, 2011; accepted April 12, 2011; published April 18, 2011.

## LITERATURE CITED

**Adam P, Hecht S, Eisenreich W, Kaiser J, Gräwert T, Arigoni D, Bacher A, Rohdich F** (2002) Biosynthesis of terpenes: studies on 1-hydroxy-2-methyl-2-(E)-butenyl 4-diphosphate reductase. Proc Natl Acad Sci USA **99:** 12108–12113

**Affek HP** (2003) Isoprene emission from plants: physiological role and

isotopic composition. PhD thesis. Weizmann Institute of Science, Rehovot, Israel

**Affek HP, Yakir D** (2002) Protection by isoprene against singlet oxygen in leaves. Plant Physiol **129:** 269–277

**Affek HP, Yakir D** (2003) Natural abundance carbon isotope composition of isoprene reflects incomplete coupling between isoprene synthesis and photosynthetic carbon flow. Plant Physiol **131:** 1727–1736

**Andre C, Froehlich JE, Moll MR, Benning CA** (2007) A heteromeric plastidic pyruvate kinase complex involved in seed oil biosynthesis in *Arabidopsis*. Plant Cell **19:** 2006–2022

**Andriotis VME, Kruger NJ, Pike MJ, Smith AM** (2010) Plastidial glycolysis in developing *Arabidopsis* embryos. New Phytol **185:** 649–662

**Bagge P, Larsson C** (1986) Biosynthesis of aromatic amino acids by highly purified spinach chloroplasts: compartmentation and regulation of the reactions. Physiol Plant **68:** 641–647

**Barta C, Loreto F** (2006) The relationship between the methyl-erythritol phosphate pathway leading to emission of volatile isoprenoids and abscisic acid content in leaves. Plant Physiol **141:** 1676–1683

**Baud S, Wuillème S, Dubreucq B, de Almeida A, Vuagnat C, Lepiniec L, Miquel M, Rochat C** (2007) Function of plastidial pyruvate kinases in seeds of *Arabidopsis thaliana*. Plant J **52:** 405–419

**Bayer RG, Stael S, Csaszar E, Teige M** (2011) Mining the soluble chloroplast proteome by affinity chromatography. Proteomics **11:** 1287–1299

**Behnke K, Ehlting B, Teuber M, Bauerfeind M, Louis S, Hänsch R, Polle A, Bohlmann J, Schnitzler JP** (2007) Transgenic, non-isoprene emitting poplars don't like it hot. Plant J **51:** 485–499

**Bennoun P** (1982) Evidence for a respiratory chain in the chloroplast. Proc Natl Acad Sci USA **79:** 4352–4356

**Bennoun P** (2001) Chlororespiration and the process of carotenoid biosynthesis. Biochim Biophys Acta **1506:** 133–142

**Bick JA, Lange BM** (2003) Metabolic cross talk between cytosolic and plastidial pathways of isoprenoid biosynthesis: unidirectional transport of intermediates across the chloroplast envelope membrane. Arch Biochem Biophys **415:** 146–154

**Brüggemann N, Schnitzler JP** (2002) Relationship of isopentenyl diphosphate (IDP) isomerase activity to isoprene emission of oak leaves. Tree Physiol **22:** 1011–1018

**Cassera MB, Merino EF, Peres VJ, Kimura EA, Wunderlich G, Katzin AM** (2007) Effect of fosmidomycin on metabolic and transcript profiles of the methylerythritol phosphate pathway in *Plasmodium falciparum*. Mem Inst Oswaldo Cruz Rio J **102:** 377–383

**Chastain CJ, Fries JP, Vogel JA, Randklev CL, Vossen AP, Dittmer SK, Watkins EE, Fiedler LJ, Wacker SA, Meinhover KC, et al** (2002) Pyruvate,orthophosphate dikinase in leaves and chloroplasts of $C_3$ plants undergoes light-/dark-induced reversible phosphorylation. Plant Physiol **128:** 1368–1378

**Chastain CJ, Xu W, Parsley K, Sarath G, Hibberd JM, Chollet R** (2008) The pyruvate, orthophosphate dikinase regulatory proteins of *Arabidopsis* possess a novel, unprecedented Ser/Thr protein kinase primary structure. Plant J **53:** 854–863

**Claeys M, Graham B, Vas G, Wang W, Vermeylen R, Pashynska V, Cafmeyer J, Guyon P, Andreae MO, Artaxo P, et al** (2004) Formation of secondary organic aerosols through photooxidation of isoprene. Science **303:** 1173–1176

**Cordoba E, Salmi M, León P** (2009) Unravelling the regulatory mechanisms that modulate the MEP pathway in higher plants. J Exp Bot **60:** 2933–2943

**Cruz JA, Emery C, Wüst M, Kramer DM, Lange BM** (2008) Metabolite profiling of Calvin cycle intermediates by HPLC-MS using mixed-mode stationary phases. Plant J **55:** 1047–1060

**Deneris ES, Stein RA, Mead JF** (1985) Acid-catalyzed formation of isoprene from a mevalonate-derived product using a rat liver cytosolic fraction. J Biol Chem **260:** 1382–1385

**Disch A, Hemmerlin A, Bach TJ, Rohmer M** (1998) Mevalonate-derived isopentenyl diphosphate is the biosynthetic precursor of ubiquinone prenyl side chain in tobacco BY-2 cells. Biochem J **331:** 615–621

**Dudareva N, Andersson S, Orlova I, Gatto N, Reichelt M, Rhodes D, Boland W, Gershenzon J** (2005) The nonmevalonate pathway supports both monoterpene and sesquiterpene formation in snapdragon flowers. Proc Natl Acad Sci USA **102:** 933–938

**Eastmond PJ, Rawsthorne S** (2000) Coordinate changes in carbon partitioning and plastidial metabolism during the development of oilseed rape embryos. Plant Physiol **122:** 767–774

**Eisenreich W, Rohdich F, Bacher A** (2001) Deoxyxylulose phosphate pathway to terpenoids. Trends Plant Sci **6:** 78–84

**Falbel TG, Sharkey TD** (2005) Determining the DMAPP that is available for isoprene synthesis. Poster 57, Secondary Metabolism. *In* Plant Biology 2005, July 16-July 20, 2005, Seattle, WA. American Society of Plant Biologists, Rockville, MD, no. 625

**Fall R, Monson RK** (1992) Isoprene emission rate and intercellular isoprene concentration as influenced by stomatal distribution and conductance. Plant Physiol **100:** 987–992

**Flores-Pérez U, Pérez-Gil J, Rodríguez-Villalón A, Gil MJ, Vera P, Rodríguez-Concepción M** (2008) Contribution of hydroxymethylbutenyl diphosphate synthase to carotenoid biosynthesis in bacteria and plants. Biochem Biophys Res Commun **371:** 510–514

**Flügge UI, Gao W** (2005) Transport of isoprenoid intermediates across chloroplast envelope membranes. Plant Biol (Stuttg) **7:** 91–97

**Flügge UI, Heldt HW** (1984) The phosphate-triose phosphate-phosphoglycerate translocator of the chloroplast. Trends Biochem Sci **9:** 530–533

**Fuentes JD, Lerdau M, Atkinson R, Baldocchi D, Bottenheim JW, Ciccioli P, Lamb B, Geron C, Gu L, Guenther A, et al** (2000) Biogenic hydrocarbons in the atmospheric boundary layer: a review. Bull Am Meteorol Soc **81:** 1537–1575

**Gerst U, Schönknecht G, Heber U** (1994) ATP and NADPH as the driving force of carbon reduction in leaves in relation to thylakoid energization by light. Planta **193:** 421–429

**Ghirardo A, Gutknecht J, Zimmer I, Brüggemann N, Schnitzler JP** (2011) Biogenic volatile organic compound and respiratory $CO_2$ emissions after $^{13}C$-labeling: online tracing of C translocation dynamics in poplar plants. PLoS ONE **6:** e17393

**Givan CV** (1999) Evolving concepts in plant glycolysis: two centuries of progress. Biol Rev Camb Philos Soc **74:** 277–309

**Hampp R, Goller M, Ziegler H** (1982) Adenylate levels, energy charge, and phosphorylation potential during dark-light and light-dark transition in chloroplasts, mitochondria, and cytosol of mesophyll protoplasts from *Avena sativa* L. Plant Physiol **69:** 448–455

**Hansel A, Jordan A, Warneke C, Holzinger R, Wisthaler A, Lindinger W** (1999) Proton-transfer-reaction mass spectrometry (PTR-MS): on-line monitoring of volatile organic compounds at volume mixing ratios of a few pptv. Plasma Sources Sci Technol **8:** 332–336

**Heber U, Neimanis S, Dietz KJ, Viil J** (1986) Assimilatory power as a driving force in photosynthesis. Biochim Biophys Acta **852:** 144–155

**Hemmerlin A, Hoeffler JF, Meyer O, Tritsch D, Kagan IA, Grosdemange-Billiard C, Rohmer M, Bach TJ** (2003) Cross-talk between the cytosolic mevalonate and the plastidial methylerythritol phosphate pathways in tobacco Bright Yellow-2 cells. J Biol Chem **278:** 26666–26676

**Hoppe P, Heintze A, Riedel A, Creuzer C, Schultz G** (1993) The plastidic 3-phosphoglycerate → acetyl-CoA pathway in barley leaves and its involvement in the synthesis of amino acids, plastidic isoprenoids and fatty acids during chloroplast development. Planta **190:** 253–262

**Hwang I, Sakakibara H** (2006) Cytokinin biosynthesis and perception. Physiol Plant **126:** 528–538

**Inoue Y, Kobayashi Y, Shibata K, Heber U** (1978) Synthesis and hydrolysis of ATP by intact chloroplasts under flash illumination and in darkness. Biochim Biophys Acta **504:** 142–152

**Ji L, Becana M, Klucas RV** (1992) Involvement of molecular oxygen in the enzyme-catalyzed NADH oxidation and ferric leghemoglobin reduction. Plant Physiol **100:** 33–39

**Joyard J, Ferro M, Masselon C, Seigneurin-Berny D, Salvi D, Garin J, Rolland N** (2010) Chloroplast proteomics highlights the subcellular compartmentation of lipid metabolism. Prog Lipid Res **49:** 128–158

**Kaiser WM, Bassham JA** (1979a) Carbon metabolism of chloroplasts in the dark: oxidative pentose phosphate cycle versus glycolytic pathway. Planta **144:** 193–200

**Kaiser WM, Bassham JA** (1979b) Light-dark regulation of starch metabolism in chloroplasts. I. Levels of metabolites in chloroplasts and medium during light-dark transition. Plant Physiol **63:** 105–108

**Kow YW, Erbes DL, Gibbs M** (1982) Chloroplast respiration: a means of supplying oxidized pyridine nucleotide for dark chloroplastic metabolism. Plant Physiol **69:** 442–447

**Kuzuyama T, Shimizu T, Takashashi S, Seto H** (1998) Fosmidomycin, a specific inhibitor of 1-deoxy-D-xylulose-5-phosphate reductoisomerase in the nonmevalonate pathway for terpenoid biosynthesis. Tetrahedron Lett **39:** 7913–7916

**Laisk A, Kiirats O, Oja V** (1984) Assimilatory power (postillumination $CO_2$ uptake) in leaves. Plant Physiol **76:** 723–729

**Laisk A, Oja V** (1998) Dynamics of Leaf Photosynthesis: Rapid-Response Measurements and Their Interpretations. CSIRO Publishing, Canberra, Australia

**Laisk A, Oja V, Rasulov B, Rämma H, Eichelmann H, Kasparova I, Pettai H, Padu E, Vapaavuori E** (2002) A computer-operated routine of gas exchange and optical measurements to diagnose photosynthetic apparatus in leaves: measurement, environmental dependencies, and kinetic properties. Plant Cell Environ **25:** 923–943

**Laisk A, Talts E, Oja V, Eichelmann H, Peterson RB** (2010) Fast cyclic electron transport around photosystem I in leaves under far-red light: a proton-uncoupled pathway? Photosynth Res **103:** 79–95

**Li Z, Ratliff EA, Sharkey TD** (2011) Effect of temperature on postillumination isoprene emission in oak and poplar. Plant Physiol **155:** 1037–1046

**Lichtenthaler HK** (1999) The 1-deoxy-D-xylulose-5-phosphate pathway of isoprenoid biosynthesis in plants. Annu Rev Plant Physiol Plant Mol Biol **50:** 47–65

**Lichtenthaler HK** (2007) Biosynthesis, accumulation and emission of carotenoids, $\alpha$-tocopherol, plastoquinone, and isoprene in leaves under high photosynthetic irradiance. Photosynth Res **92:** 163–179

**Lindinger W, Hansel A, Jordan A** (1998) Proton-transfer-reaction mass spectrometry (PTR-MS): on-line monitoring of volatile organic compounds at pptv levels. Chem Soc Rev **27:** 347–354

**Loivamäki M, Louis S, Cinege G, Zimmer I, Fischbach RJ, Schnitzler JP** (2007) Circadian rhythms of isoprene biosynthesis in grey poplar leaves. Plant Physiol **143:** 540–551

**Loivamäki M, Mumm R, Dicke M, Schnitzler JP** (2008) Isoprene interferes with the attraction of bodyguards by herbaceous plants. Proc Natl Acad Sci USA **105:** 17430–17435

**Loreto F, Ciccioli P, Brancaleoni E, Frattoni M, Delfine S** (2000) Incomplete $^{13}C$ labelling of $\alpha$-pinene content of *Quercus ilex* leaves and appearance of unlabelled C in $\alpha$-pinene emission in the dark. Plant Cell Environ **23:** 229–234

**Loreto F, Sharkey TD** (1990) A gas-exchange study of photosynthesis and isoprene emission in *Quercus rubra* L. Planta **182:** 523–531

**Loreto F, Sharkey TD** (1993) On the relationship between isoprene emission and photosynthetic metabolites under different environmental conditions. Planta **189:** 420–424

**Loreto F, Velikova V** (2001) Isoprene produced by leaves protects the photosynthetic apparatus against ozone damage, quenches ozone products, and reduces lipid peroxidation of cellular membranes. Plant Physiol **127:** 1781–1787

**Mahmoud SS, Croteau RB** (2002) Strategies for transgenic manipulation of monoterpene biosynthesis in plants. Trends Plant Sci **7:** 366–373

**Mair T, Warnke C, Tsuji K, Müller SC** (2005) Control of glycolytic oscillations by temperature. Biophys J **88:** 639–646

**Mgalobilishvili MP, Khetsuriani ND, Kalandadze AN, Sanadze GA** (1978) Localization of isoprene biosynthesis in poplar leaf chloroplasts. Fiziol Rast **25:** 1055–1061

**Monson RK, Fall R** (1989) Isoprene emission from aspen leaves: influence of environment and relation to photosynthesis and photorespiration. Plant Physiol **90:** 267–274

**Monson RK, Hills AJ, Zimmerman PR, Fall RR** (1991) Studies of the relationship between isoprene emission rate and $CO_2$ or photon-flux density using a real-time isoprene analyser. Plant Cell Environ **14:** 517–523

**Muñoz-Bertomeu J, Cascales-Miñana B, Mulet JM, Baroja-Fernández E, Pozueta-Romero J, Kuhn JM, Segura J, Ros R** (2009) Plastidial glyceraldehyde-3-phosphate dehydrogenase deficiency leads to altered root development and affects the sugar and amino acid balance in Arabidopsis. Plant Physiol **151:** 541–558

**Niinemets Ü, Monson RK, Arneth A, Ciccioli P, Kesselmeier J, Kuhn U, Noe SM, Peñuelas J, Staudt M** (2010) The leaf-level emission factor of volatile isoprenoids: caveats, model algorithms, response shapes and scaling. Biogeosciences **7:** 1809–1832

**Nixon PJ** (2000) Chlororespiration. Philos Trans R Soc Lond B Biol Sci **35:** 1541–1547

**Ogrel OD, Fegeding KV, Kapreliants AS, Lysak EI, Ngo MS, Sudarikov AB, Karatian EF, Ostrovskiĭ DN** (1996) [Participation of 2-C-methyl-D-erythritol-2,4-cyclopyrophosphate in reactions of bacteria on oxidative stress and their persistence in macrophages]. Biokhimiia **61:** 1294–1302

**Ostrovsky D, Amirov R, Kharatian E, Ogrel O, Stepanov S, Sibeldina L, Shipanova I, Taptykova S** (1994) Bacteria and pesticides: a new aspect of interaction. Involvement of a new biofactor. Biofactors **4:** 151–154

**Page JE, Hause G, Raschke M, Gao W, Schmidt J, Zenk MH, Kutchan TM** (2004) Functional analysis of the final steps of the 1-deoxy-D-xylulose 5-phosphate (DXP) pathway to isoprenoids in plants using virus-induced gene silencing. Plant Physiol **134:** 1401–1413

**Pastenes C, Horton P** (1996) Effect of high temperature on photosynthesis in beans. II. $CO_2$ assimilation and metabolite contents. Plant Physiol **112:** 1253–1260

**Pearcy RW** (1988) Photosynthetic utilisation of lightflecks by understory plants. Aust J Plant Physiol **15:** 223–238

**Pearcy RW, Gross LJ, He D** (1997) An improved dynamic model of photosynthesis for estimation of carbon gain in sunfleck light regimes. Plant Cell Environ **20:** 411–424

**Peltier G, Cournac L** (2002) Chlororespiration. Annu Rev Plant Biol **53:** 523–550

**Ramachandra RA, Das VSR** (1987) Chloroplast autonomy for the biosynthesis of isopentenyl diphosphate in guayule (*Parthenium argentatum* Gray). New Phytol **106:** 457–464

**Ramos-Valdivia AC, van der Heijden R, Verpoorte R** (1997) Isopentenyl diphosphate isomerase: a core enzyme in isoprenoid biosynthesis. A review of its biochemistry and function. Nat Prod Rep **14:** 591–603

**Rasulov B, Copolovici L, Laisk A, Niinemets Ü** (2009a) Postillumination isoprene emission: in vivo measurements of dimethylallyldiphosphate pool size and isoprene synthase kinetics in aspen leaves. Plant Physiol **149:** 1609–1618

**Rasulov B, Hüve K, Bichele I, Laisk A, Niinemets Ü** (2010) Temperature response of isoprene emission in vivo reflects a combined effect of substrate limitations and isoprene synthase activity: a kinetic analysis. Plant Physiol **154:** 1558–1570

**Rasulov B, Hüve K, Välbe M, Laisk A, Niinemets Ü** (2009b) Evidence that light, carbon dioxide, and oxygen dependencies of leaf isoprene emission are driven by energy status in hybrid aspen. Plant Physiol **151:** 448–460

**Rivasseau C, Seemann M, Boisson AM, Streb P, Gout E, Douce R, Rohmer M, Bligny R** (2009) Accumulation of 2-C-methyl-D-erythritol 2,4-cyclodiphosphate in illuminated plant leaves at supraoptimal temperatures reveals a bottleneck of the prokaryotic methylerythritol 4-phosphate pathway of isoprenoid biosynthesis. Plant Cell Environ **32:** 82–92

**Rodríguez-Concepción M** (2006) Early steps in isoprenoid biosynthesis: multilevel regulation of the supply of common precursors in plant cells. Phytochem Rev **5:** 1–15

**Rodríguez-Concepción M, Boronat A** (2002) Elucidation of the methylerythritol phosphate pathway for isoprenoid biosynthesis in bacteria and plastids: a metabolic milestone achieved through genomics. Plant Physiol **130:** 1079–1089

**Rodríguez-Concepción M, Forés O, Martinez-García JF, González V, Phillips MA, Ferrer A, Boronat A** (2004) Distinct light-mediated pathways regulate the biosynthesis and exchange of isoprenoid precursors during *Arabidopsis* seedling development. Plant Cell **16:** 144–156

**Rohdich F, Wungsintaweekul J, Fellermeier M, Sagner S, Herz S, Kis K, Eisenreich W, Bacher A, Zenk MH** (1999) Cytidine 5′-triphosphate-dependent biosynthesis of isoprenoids: YgbP protein of *Escherichia coli* catalyzes the formation of 4-diphosphocytidyl-2-C-methylerythritol. Proc Natl Acad Sci USA **96:** 11758–11763

**Ruuska S, Andrews TJ, Badger MR, Hudson GS, Laisk A, Price GD, von Caemmerer S** (1998) The interplay between limiting processes in $C_3$ photosynthesis studied by rapid-response gas exchange using transgenic tobacco impaired in photosynthesis. Aust J Plant Physiol **25:** 859–870

**Sanadze GA** (1966) Biosynthesis and light-dependent isoprene emission from leaves. Doctor of Science thesis. Institute of Plant Physiology, Moscow

**Sanadze GA, Baazov DI** (1985) Usileniye fotosinteza i vyhoda izoprena u listyev topolya [Enhancement of photosynthesis and isoprene emission in poplar leaves]. Soobshch Akad Nauk Gruz SSR **118:** 597–600

**Schwender J, Gemünden C, Lichtenthaler HK** (2001) Chlorophyta exclusively use the 1-deoxyxylulose 5-phosphate/2-C-methylerythritol 4-phosphate pathway for the biosynthesis of isoprenoids. Planta **212:** 416–423

**Schwender J, Müller C, Zeidler J, Lichtenthaler HK** (1999) Cloning and heterologous expression of a cDNA encoding 1-deoxy-D-xylulose-

5-phosphate reductoisomerase of *Arabidopsis thaliana*. FEBS Lett **455:** 140–144

**Seemann M, Rohmer M** (2007) Isoprenoid biosynthesis via the methylerythritol phosphate pathway: GcpE and LytB, two novel iron-sulphur proteins. C R Chim **10:** 748–755

**Seemann M, Tse Sum Bui B, Wolff M, Miginiac-Maslow M, Rohmer M** (2006) Isoprenoid biosynthesis in plant chloroplasts via the MEP pathway: direct thylakoid/ferredoxin-dependent photoreduction of GcpE/IspG. FEBS Lett **580:** 1547–1552

**Sharkey TD, Seemann JR, Pearcy RW** (1986) Contribution of metabolites of photosynthesis to postillumination $CO_2$ assimilation in response to lightflecks. Plant Physiol **82:** 1063–1068

**Sharkey TD, Singsaas EL** (1995) Why plants emit isoprene. Nature **374:** 769

**Sharkey TD, Wiberley AE, Donohue AR** (2008) Isoprene emission from plants: why and how. Ann Bot (Lond) **101:** 5–18

**Silver GM, Fall R** (1995) Characterization of aspen isoprene synthase, an enzyme responsible for leaf isoprene emission to the atmosphere. J Biol Chem **270:** 13010–13016

**Stitt M, ap Rees T** (1979) Capacities of pea chloroplasts to catalyse the oxidative pentose phosphate pathway and glycolysis. Phytochemistry **18:** 1905–1911

**Stitt M, Heldt HW** (1981) Physiological rates of starch breakdown in isolated intact spinach chloroplasts. Plant Physiol **68:** 755–761

**Stitt M, Wirtz W, Gerhardt R, Heldt HW, Spencer CA, Walker D, Foyer C** (1985) A comparative study of metabolite levels in plant leaf material in the dark. Planta **166:** 354–364

**Troncoso-Ponce MA, Kruger NJ, Ratcliffe G, Garcés R, Martínez-Force E** (2009) Characterization of glycolytic initial metabolites and enzyme activities in developing sunflower (*Helianthus annuus* L.) seeds. Phytochemistry **70:** 1117–1122

**Tuttle SW, Maity A, Oprysko PR, Kachur AV, Ayene IS, Biaglow JE, Koch CJ** (2007) Detection of reactive oxygen species via endogenous oxidative pentose phosphate cycle activity in response to oxygen concentration: implications for the mechanism of HIF-1alpha stabilization under moderate hypoxia. J Biol Chem **282:** 36790–36796

**Vahala J, Keinänen M, Schützendübel A, Polle A, Kangasjärvi J** (2003) Differential effects of elevated ozone on two hybrid aspen genotypes predisposed to chronic ozone fumigation: role of ethylene and salicylic acid. Plant Physiol **132:** 196–205

**Vickers CE, Gershenzon J, Lerdau MT, Loreto F** (2009) A unified mechanism of action for volatile isoprenoids in plant abiotic stress. Nat Chem Biol **5:** 283–291

**Vickers CE, Possell M, Hewitt CN, Mullineaux PM** (2010) Genetic structure and regulation of isoprene synthase in poplar (*Populus* spp.). Plant Mol Biol **73:** 547–558

**Vickers CE, Possell M, Laothawornkitkul J, Ryan AC, Hewitt CN, Mullineaux PM** (April 7, 2011) Isoprene synthesis in plants: lessons from a transgenic tobacco model. Plant Cell Environ http://dx.doi.org/10.1111/j.1365-3040.2011.02303.x

**Voll LM, Hajirezaei MR, Czogalla-Peter C, Lein W, Stitt M, Sonnewald U, Börnke F** (2009) Antisense inhibition of enolase strongly limits the metabolism of aromatic amino acids, but has only minor effects on respiration in leaves of transgenic tobacco plants. New Phytol **184:** 607–618

**Yamada M, Nakamura Y** (1975) Fatty acid synthesis by spinach chloroplasts. II. The path from PGA to fatty acids. Plant Cell Physiol **16:** 151–162

**Zeidler JG, Schwender J, Müller C, Wiesner J, Weidemeyer C, Beck E, Jomaa H, Lichtenthaler HK** (1998) Inhibition of the non-mevalonate 1-deoxy-d-xylulose-5-phosphate pathway of plant isoprenoid biosynthesis by fosmidomycin. Z Naturforsch Sect C Biosci **53c:** 980–986

**Zepeck F, Gräwert T, Kaiser J, Schramek N, Eisenreich W, Bacher A, Rohdich F** (2005) Biosynthesis of isoprenoids. purification and properties of IspG protein from *Escherichia coli*. J Org Chem **70:** 9168–9174